

Manuscript refereed by Professor Luis Llanes (Catalunya Universitat Politècnica, Spain)

Precipitation of Intermetallic Phases in Coarse-Grained Hardmetals by Low-Temperature Annealing

S. Wawrzik¹, C. Buchegger¹, W. Lengauer^{1,*}, H. van den Berg², K. Rödiger², M. Wolf³, A. Helldörfer³, J. Bernardi⁴, J. Gruber⁴

¹ Vienna University of Technology, Getreidemarkt 9/164CT, A-1060 Vienna, Austria

² Kennametal Shared Services GmbH, Münchener Straße 125-127, D-45145 Essen, Germany

³ Kennametal Shared Services GmbH, Eckersdorfer Straße 10, D-95490 Mistelgau, Germany

⁴ Vienna University of Technology, USTEM, Wiedner Hauptstraße 8-10, A-1040 Vienna, Austria

* corresponding author: walter.lengauer@tuwien.ac.at

Abstract

Binder-phase modification was performed by annealing of coarse-grained WC-15%Co hardmetal grades used for rock-drilling, mining and road construction. Technically applicable, short annealing cycles were applied to low-C hardmetals in order to cause precipitation of intermetallic phases in the Co binder. Detailed TEM investigations showed that the precipitations consist of Co_3W (at higher annealing temperatures) or closely-related precursors thereof (at lower annealing temperatures). The presence of the Co_3W phase was also confirmed by XRD and a Rietveld analysis yielded an amount of 0.5% wt%. The hardmetals were further characterised by SEM, Vickers hardness (HV30), coercive force (H_c) and magnetic saturation measurements, bending strength (TRS) and erosive mass loss. H_c increased upon precipitation of intermetallic phases whereas the WC grain size remained unchanged. For moderate annealing conditions of a short period at low temperatures TRS and hardness remained unchanged but the erosive resistance increased by ~12%.

1. Introduction

As tool materials, coarse-grained hardmetals are widely used for rock-drilling, mining and road construction. They combine high toughness with high impact resistance. The lifetime of such tools is determined by wear. Therefore, the aim is to reduce the mass loss. An idea to achieve this goal is the strengthening of the hardmetal binder.

Between the 1960s and 1980s extensive investigations on the mechanism of the precipitation of intermetallic phases from W-supersaturated Co binder in model alloys [1,2] and hardmetals [3-6] were conducted by annealing experiments of up to 500 h. Depending on the annealing temperature different shapes of these precipitations, not all of which could be characterised structurally, were reported [5]: coherent precipitations of $\varnothing = 3 - 5$ nm are formed at 550 – 600°C, coherent precipitations of $\varnothing = 15$ nm, partially grown to lamellae at 650°C; coherent precipitations ($\varnothing = 30$ nm) in form of lamellae, plates and Co_3W form at 700°C, and at 750°C lamellae and plate-shaped Co_3W .

Jonsson [1,3,4] investigated the behaviour of WC-Co hardmetals with 11 wt% and 25 wt% Co, respectively, during heat-treatment at 650°C [3] and 950°C [4]. After sintering, the Co binder contained about 6 wt% W as supersaturated solid solution. TEM investigations showed that a highly dispersed coherent metastable α' -phase (ordered structure of the fcc Co) forms during annealing at 650°C (dwell time 165 h) in the fcc Co binder. By XRD the presence of this α' -phase could not be demonstrated. In hardmetals annealed significantly longer than 160 h Co_3W was, however, detected by XRD. Hcp Co and Co_3W should have formed, but were not observed by SEM or TEM. ϵ -Co predominates in the binder at a low carbon content [1] and thus it was assumed [3,4] that a high carbon content inhibits the formation of ϵ -Co and Co_3W .

Euro PM2015 – Hard Materials - Processing 2

Grewe [6] found that the hardness as well as the coercivity had a maximum during annealing, whereas the maximum of the coercivity occurred always at shorter annealing times than that maximum of hardness. At the annealing time of either maximum no Co_3W was formed. In both cases substructures which can be considered as precursors of Co_3W are responsible for the increase. Because the coercivity is sensitive to minimal changes in the substructures and the hardness to coarsened substructures the maxima are separated from to each other. Metal-cutting wear tests show that an annealing process at 650°C for 100 h or 200 h, respectively, can decrease the flank wear and crater wear by about 20 – 25% [6,7]. In case of toughness no improvement was achieved [8].

Tillwick and Joffe [9] described precipitation, aging and redissolution processes in a hardmetal grade with 25 wt% Co by observing changes in saturation magnetisation (σ_s). At ageing at 1000°C σ_s decreased. From that they have concluded that W and carbon dissolved in the binder (in the WC/Co system σ_s decreases linearly with increasing W content in the Co binder [10]). The solubility of W and C in the binder increases with increasing temperature. The W solubility is 27wt% at 1000°C and 12 wt% at 700°C , the C solubility at 1000°C is 1.6 wt% C, while at 700°C it is almost zero. If after aging at 1000°C a second aging at 700°C was performed the supersaturated solid solution precipitated Co_3W and saturation magnetisation leaped up. A further aging at 1000°C led again to decreasing of σ_s , i.e. the process was observed to be reversible. It was expected that the precipitation of Co_3W might take place at the interfaces between WC and Co but it could not be detected by microscopic observations nor by XRD [9].

Freytag et al. [11] investigated WC-Co hardmetals by magnetic measurements at different carbon contents. Upon comparison with data of [9] they realised that the insertion of W in non-ferromagnetic Co_3W reduces the magnetic saturation not as strong as W dissolved in Co. Hence, they concluded that a part of W had to form an intermetallic paramagnetic phase Co_3W .

In the binary Co-W system, hexagonal Co is in equilibrium with Co_3W at low temperatures and has little solubility for W [12]. For Co-W alloys, Carvalho et al. [13] described a continuous, displacive Widmannstätten-type precipitation of Co_3W in supersaturated fcc Co via hcp Co, as well as a peritectoid formation from supersaturated fcc Co + Co_7W_6 at 1093°C . If carbon is added to Co-W, it stabilises fcc Co so no hexagonal phase exists and no Co_3W forms in C-Co-W alloys at high carbon level.

Generally, the formation of intermetallic phases in hardmetals decreases their TRS [3,14] and increases the hardness of the binder phase [14]. Latest investigations published by Konyashin et al. [15] proved the existence of Co_3W nano-sized needles (10 – 40 nm) in WC-10 wt%Co hardmetals and low carbon content (5.75 wt% C) annealed at 800°C for 20 h. HRTEM investigations show that these needles are embedded in hcp Co (ϵ -Co). The phases Co_3W and ϵ -Co were well aligned to each other. Compared to unannealed samples the hardness increased by 10% whereas the TRS and the fracture toughness decreased by about 15% and 25%, caused by the embrittled binder. They also investigated samples with medium carbon content (6 wt%) annealed at 600°C for 10 h with TEM and found extremely fine nanoparticles (3 nm) with the Cu_3Au structure type, embedded in fcc Co. Because of the small size the chemical composition could not be analysed. This metastable phase is fully coherent to the fcc Co. With these hardmetals the lifetime of road-planing picks was reported to increase by 2-3x [15].

2. Experimental

2.1 Sample preparation

For the preparation of laboratory grades of hardmetals, a WC powder with mean grain size of 8 μm was employed. For precise adjustment of the carbon level, carbon black and W powder was used. After weighting, the powder mixtures WC-15%Co were ball milled with cyclohexane for 24 h. The powder-to-ball mass ratio was 10:1. The powder mixtures were pressed uniaxially with 350 MPa without pressing aid.

The samples were sintered and then low-temperature annealed (schematically given in Tab. 1).

Tab. 1: Annealing processes ($T < 900^{\circ}\text{C}$, $t < 6\text{h}$)

Name	Temperature	Time
A	unannealed	
B	low	short
C	high	long

The same raw materials were employed for preparation of industrial grades. These grades were subjected to identical annealing steps and employed for TRS measurements.

2.2 Sample characterisation

For metallographic inspection the samples were cut, ground and polished with 1 μm diamond paste for light optical and scanning electron microscopy. Vickers hardness (HV30) testing followed DIN ISO 3878. All individual samples were subjected to measurement of magnetic saturation and coercive force.

For TEM microstructure analysis in a FEI TECNAI F20 transmission electron microscope lamellae were prepared by FIB (focused ion beam) preparation in a DualBeam-FIB FEI Quanta 200 FEGSEM 3D electron microscope. No additional preparation was necessary for TEM investigations. Elemental analysis was made by EDX and EELS (electron energy loss spectroscopy) case-by-case.

For XRD solid samples were cut, ground and polished before measurement with Ni-filtered Co-K_{α} radiation. The step width was 0.02° (Θ) in the range of $5 - 70^{\circ}$ (Θ) with sample rotation. For Rietveld analysis the software Topas was used.

For TRS measurement, about 20 hardmetal bars (20x6.5x5.25 mm) were subjected to a three-point bending tests according to DIN ISO 3327 with a following Weibull analysis.

The erosion resistance was measured with a sandblasting test, inspired by the ASTM C704 [16] standard. This is a jet abrasion test covering the determination of relative abrasion resistance of a sample at room temperature. As an abrasive we used 100 g of Al_2O_3 powder with 125 – 180 μm particle size at 2 bar air-jet pressure. A boron carbide nozzle with 1.5 mm diameter was used at a distance of 12 mm. For each single test fresh Al_2O_3 powder of a single batch was employed. The erosion resistance of the hardmetal was quantified by mass-loss measurement (Δg). The mean deviation of mass loss of five parallel tests amounts about $\pm 0.2\%$.

3. Results and discussion

3.1 SEM microstructure analysis

SEM investigations (Fig. 1) of annealed samples with low carbon content show structured areas in the binder whereas the binder of unannealed samples is unstructured (Fig. 1a). All tested samples had the same magnetic saturation before low-temperature annealing.

The amount of structured area in the binder increases with time and the intensity of structures increases with temperature. The sample annealed with annealing process B shows just some areas with weakly structured binder (Fig. 1b) whereas the sample annealed with annealing process C shows intense, clearly visible structures (Fig. 1c). These structures were found in samples with a low carbon level and are similar to that described by Wirmark and Dunlop [2].

3.2 TEM investigations

First, the sample annealed with annealing process C was chosen, because it shows the most intensive structures in SEM investigations (Fig. 1c).

In the first step, EDX analysis in the four areas marked in Fig. 2a were made. Area 1 is situated in the binder phase, area 2 in WC and areas 3 and 4 in the striated lamellae. The results of the EDX analysis

are given in Tab.2. Although EDX has a restricted accuracy it can be seen that the composition of the Co_3W phase is located between WC and that of the binder.

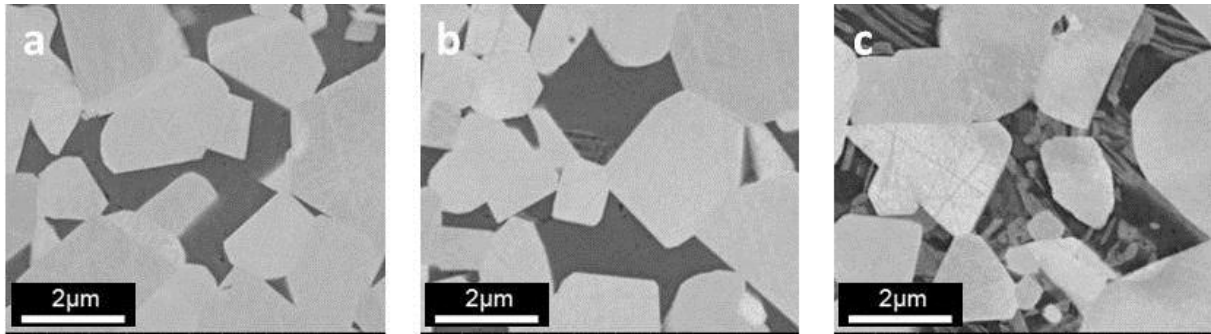


Fig. 1, a: unannealed (A), b: low T - short t (B), c: high T - long t (C), SEM-BSE, magn. 40,000x.

Dark field image and HRTEM analysis (to be presented elsewhere) showed segregation between heavy and light elements within the lamellae. No lattice plane distortion and no additional reflection could be identified in the diffraction pattern. Consequently, these segregations are high-coherent precipitations with the same crystal structure.

Upon analysis of the diffraction pattern (software JEMS) of the lamellae best agreement to the lattice spacings of Co_3W [17], space group $P6_3/mmc$ could be found.

Tab. 2: EDX analysis results (mol%) for areas indicated in Fig.2a

Area	C	Co	W	Phase
1	4.8	92.0	3.2	Co
2	36.7	2.8	60.5	WC
3	8.0	74.9	17.1	Co_3W
4	12.2	69.5	18.3	Co_3W

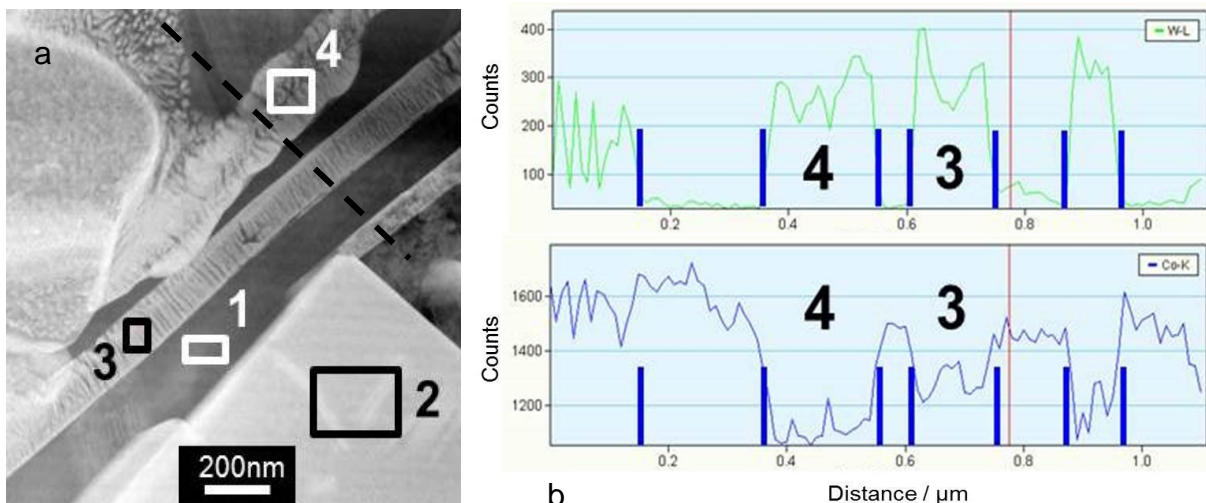


Fig. 2, a: areas and line scan position for EDX analysis, b: Line scans (top: W, bottom: Co) across three lamellae (3, 4 and one additional not indicated in Fig.2a).

Another TEM investigation was made of the sample annealed with annealing process B with only faint structures in the binder (Fig. 1b). Fig. 3a shows a TEM image of this sample. In the binder (light grey) crossed bands are visible. An EELS line scan across one of these bands is shown in Fig. 3b (W cannot be measured with EELS, therefore just C and Co are plotted). Within the band (marked with blue vertical lines) the Co content decreases as compared to the binder. From this fact and because of the darker colour of the band a W enrichment within the band can be assumed.

The structures in samples annealed with process B (Fig. 1b) are less pronounced than with annealing process C (Fig. 1c) but are certainly related to the Co_3W phase and are probably a precursor state of the latter (named ε' by Jonsson and Aronsson [1]). The indexing of the reflections representing the bands was in best agreement with those of Co_3W .

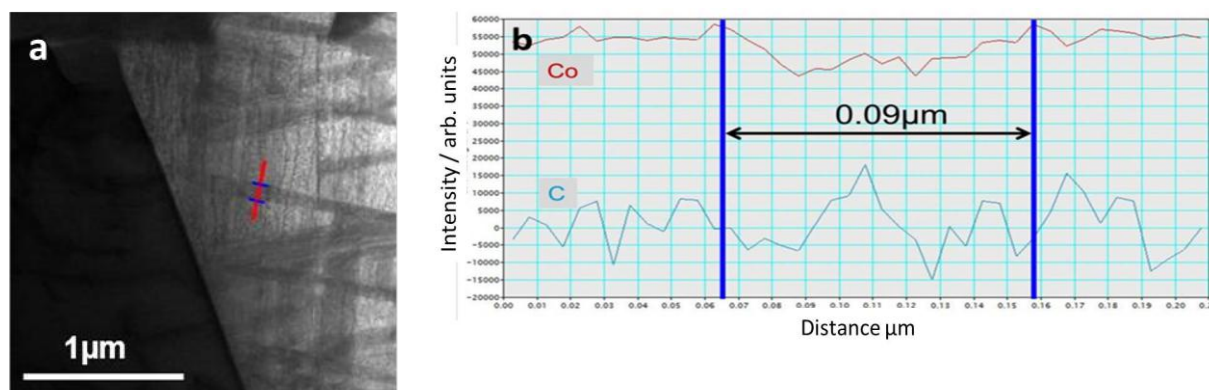


Fig. 3, a: TEM image of sample B, EELS line scan is marked, b: EELS line scan, sample annealed with annealing process B

In published isothermal sections of the system W-C-Co, for example those of Åkesson [18], WC+Co is not in equilibrium with Co_3W . These diagrams, however, were established for much higher temperatures than the investigated re-annealing temperatures. At lower temperatures the phase equilibria could change. Nevertheless, in the binary system W-Co the Co_3W phase is in equilibrium with hexagonal ε -Co, which has little solubility for W at low temperatures [12].

3.3 Rietveld analysis

The sample annealed with annealing process C was subjected to XRD / Rietveld refinement (Tab. 3). The total binder content found by this refinement (16.3 wt%) is in good agreement with the overall Co content of the hardmetal (15.0 wt%). In the binder, a huge amount of hexagonal ε -Co phase was found (almost 84% of the binder) and only a minor amount of fcc Co (ca. 13% of the binder). The content of Co_3W was found to be 0.5% of the total sample which is ca. 3% of the binder. The unit cell of fcc Co was smaller than given in literature whereas the hexagonal ε -Co lattice parameters and those of Co_3W are strikingly larger. The lattice parameters of WC are just slightly increased in comparison to literature values.

3.4 Magnetic and mechanical properties

The Vickers hardness (HV30), the coercivity (H_c) and the bending strength (TRS) of the unannealed sample (Grade A) and the annealed samples (Grades B and C) are listed in Tab. 4 together with the erosive mass loss. The erosive mass loss decreases significantly with the formation of Co_3W (Grade C) or its precursor (Grade B), whereas the hardness and TRS remains constant for Grade B.

A strong increase of H_c for samples annealed with annealing process C was found and is due to the precipitations in the binder. These precipitations shorten the mean free path and consequently the Weiss domains decrease so that H_c increases. Grade B shows only a slight increase because of the much lower amount of Co_3W (see Fig. 1b).

Tab. 3: Results of Rietveld analysis of the sample annealed with annealing process C

Lattice parameters	Sample, Å	Literature data [19], Å
a WC	2.9114	2.90631(9)
c WC	2.8436	2.83754(8)
a Co ₃ W	5.1588	5.12
c Co ₃ W	4.1589	4.12
a Co _{hcp}	2.5348	2.5031(5)
c Co _{hcp}	4.1215	4.0605(8)
a Co _{cub}	3.5340	3.5447
Phase concentration		
wt% WC	83.7	
wt% Co ₃ W	0.5	
wt% Co _{hcp}	13.7	
wt% Co _{cub}	2.1	

This is in accordance with several studies, e.g. [2,3,11], who assumed or proofed the formation of an intermetallic paramagnetic phase (Co₃W). At low C concentration such as adjusted in this work, the amount of hexagonal ϵ -Co is larger than at high carbon level, because of the C stabilises fcc Co. If we adjusted a higher carbon level, corresponding to $\sigma_S = 85\%$ of that of Co, Co₃W was no more present.

Tab. 4: Properties of the hardmetals used for TEM (Grade B, C) and as-sintered Grade A

Grade	Hardness HV30	Erosive mass loss mg	H _c kAm ⁻¹	TRS MPa
A	1190	56.0	9.4	3710
B	1180	49.0	9.8	3720
C	1130	48.9	13.5	3560

The intensive formation of Co₃W reduces TRS in Grade C (Tab. 5) in accordance with the findings of other authors, e.g. [2,14,15]. Contrary, we have not detected a hardness increase, rather a small decrease, upon this heat treatment. Thus, we assume that the hardness contribution of the modified binder phase (compare [14]) to the overall hardness is small. However, an indication for that is the finding of a substantial reduction in erosive mass loss. Obviously, the precipitations in the binder cause a hardening effect and prevent the WC grains to be extracted from the hardmetal, which is the usual failure mechanism of erosion.

The best conditions (proofed for several similar conditions such as employed for Grade B) are, however, a lower annealing temperature with shorter time (Tab. 4, Grade B), in which HV and TRS remain unchanged, but yield a similar substantial reduction in erosive mass loss. As proofed by TEM, these moderate re-annealing conditions – which could also implemented in the sintering profile – cause much finer Co₃W or precursors thereof.

The reason why in our experiments the Co₃W formation was achieved within much shorter annealing times than in most other studies (e.g. some report 25 – 100 h [2] or even several hundred hours [5]) could be due to differences in C activity of the alloys. We observed these precipitation only at low C activity close to the WC+Co+ η boarder. It is also interesting to note, that Tillwick and Joffe [9] have found an MS discontinuity at 35 min annealing time in samples annealed at 700°C and suggested that an intermediate phase forms (probably ϵ') which then transforms into Co₃W upon further annealing. A similar phenomenon was described by Jonsson and Aronsson [1] for 550-650°C but ϵ' and Co₃W occurred only at annealing times ≥ 10 h in Co-W-C alloys containing free WC.

4. Conclusion

The precipitation of Co_3W phase from W-supersaturated binder in hardmetals was already observed in the 1960s –1980s [1-5,9,14]. However, most of the annealing times of up to 500 h were clearly too long for an economical industrial use. The results of the present work show indeed clearly, that the formation of Co_3W phase or their fine precursor state (ϵ') occurs also in industrial samples at significantly shorter annealing times, leaving hardness and TRS unchanged, but increasing the erosion resistance. An implementation of such a procedure into a commercial fabrication process will widen the potential of such hardmetals.

References

- [1] Jonsson H, Aronsson B. Microstructure and hardness of cobalt-rich Co-W-C alloys after ageing in the temperature range 400-1000°C. *J Inst Met* 1969;97:281-8
- [2] Wirmark G, Dunlop GL. Phase transformation in the binder phase of Co-W-C cemented carbides. In: *Proceedings of the International Conference Science of Hard Materials* 1983:311-28
- [3] Jonsson H. Studies of the binder phase in WC-Co cemented carbides heat-treated at 650°C. *Powder Metall* 1972;15(29):1-10
- [4] Jonsson H. Studies of the binder phase in WC-Co cemented carbides heat-treated at 950°C. In: *Planseeberichte für Pulvermetallurgie* 23, vol.1; 1975:37-55
- [5] Schlump W, Kolaska J, Grewe H. Metallkundliche Untersuchungen zum Ausscheidungsverhalten in der Bindephase von WC-Co-Legierungen. *Metall* 1982;36(5):535-40
- [6] Grewe H, Kolaska J, Schlump W. Untersuchungen zum Ausscheidungsverhalten in der Bindephase von Legierungen des Systems WC-TiC-(Ta,Nb)C-Co. *Metall* 1983;37(5):485-95
- [7] Rüdiger O. Das Bindemetall – ein Problem der Hartmetallforschung. *Powd Metall Int* 1983;15:4-7.
- [8] Maritzen W. Wärmebehandlung von WC-(Ti,Ta,Nb)C-Co Hartmetallen. Technische Universität Wien, Thesis 1987.
- [9] Tillwick DL, Joffe I. Precipitation and magnetic hardening in sintered WC-Co composite materials. *J Phys D: Appl Phys* 1973;6:1585-97.
- [10] Roebuck B. Magnetic moment (saturation) measurements on hardmetals. *Int J Refract Metal Hard Mater* 1996;14(5-6):419–24.
- [11] Freytag J, Walter P, Exner HE. Charakterisierung der Binderphase von WC-Co Hartmetallen über magnetische Eigenschaften. *Z Metallkd* 1978;69(8):546-9.
- [12] MTDATA. Calculated Co-W phase diagram. MTDATA – Phase Diagram Software from the National Physical Laboratory 2010. <http://resource.npl.co.uk/mtdata/phdiagrams/cow.htm>
- [13] Carvalho PA, Bronsveld PM, Kooi BJ, De Hosson J. On the fcc->D019 transformation in C-W alloys. *Acta Mater* 2002;50(18):4511-26.
- [14] Suzuki H, Kubota H. The influence of binder phase composition on the properties of WC-Co cemented carbides. *Planseeberichte für Pulvermetallurgie* 1966;14:96-109.
- [15] Konyashin I, Lachmann F, Mazilkin AA, Straumal BB, Kübel C, Llanes, L, Baretzky, B. Strengthening zones in the Co matrix of WC-Co cemented carbides. *Scripta Mater* 2014;83:17-20.
- [16] ASTM C704 Standard Test Method for Abrasion Resistance of Refractory Materials at Room Temperature. 2014; ASTM International.
- [17] Magneli A, Westgren A. Röntgenuntersuchung von Kobalt-Wolfram Legierungen. *Z Anorg Allg Chem* 1938;238(2-3):268-72.
- [18] Åkesson L. An experimental and thermodynamic study of the Co-W-C system in the temperature range 1473-1698 K. Thesis. Uppsala University Sweden 1982.
- [19] International Centre for Diffraction Data - ICDD, WC: 51-0939, Co_3W : 02-1298, Co cub: 15-0806, Co hex: 05-0727.